

Communication

# A Zn-MOF-Catalyzed Terpolymerization of Propylene Oxide, CO<sub>2</sub>, and β-butyrolactone

Sudakar Padmanaban <sup>1</sup>, Sivanesan Dharmalingam <sup>2</sup> and Sungho Yoon <sup>1,\*</sup>

<sup>1</sup> Department of Applied Chemistry, Kookmin University, Seoul 02707, Korea; chemsuda@kookmin.ac.kr

<sup>2</sup> Greenhouse Gas Laboratory, Korea Institute of Energy Research, 152, Gajeong-ro, Yuseong-gu, Daejeon 34129, Korea; sivachem83@gmail.com

\* Correspondence: yoon@kookmin.ac.kr; Tel.: +82-02-910-4763

Received: 22 August 2018; Accepted: 11 September 2018; Published: 13 September 2018



**Abstract:** The terpolymerization of propylene oxide (PO), CO<sub>2</sub>, and a lactone is one of the prominent sustainable procedures for synthesizing thermoplastic materials at an industrial scale. Herein, the one-pot terpolymerization of PO, CO<sub>2</sub>, and β-butyrolactone (BBL) was achieved for the first time using a heterogeneous nano-sized catalyst: zinc glutarate (ZnGA-20). The reactivity of both PO and BBL increased with the CO<sub>2</sub> pressure, and the polyester content of the terpolymer poly(carbonate-co-ester) could be tuned by controlling the infeed ratio of PO to BBL. When the polyester content increased, the thermal stability of the polymers increased, whereas the glass transition temperature ( $T_g$ ) decreased.

**Keywords:** heterogeneous catalysis; metal-organic frameworks; zinc glutarate; terpolymerization; CO<sub>2</sub>; β-butyrolactone; biodegradable polymers; poly(alkylene carbonates); poly(hydroxybutyrates)

## 1. Introduction

The conversion of CO<sub>2</sub> into chemical commodities, particularly the synthesis of biodegradable poly(alkylene carbonates) by the alternating copolymerization of an epoxide and CO<sub>2</sub>, is regarded as one of the most sustainable approaches for the use of CO<sub>2</sub> as a source material in large-scale industrial processes [1–11]. Poly(alkylene carbonates) are characterized by a variety of properties, e.g., lightness, strength, durability, high transparency, heat resistance, and good electrical insulating ability. They are applied as adhesives, coating and packing materials, and binders in ceramic industries. Furthermore, they are important candidates for biomedical applications because of their low toxicity, biocompatibility, and biodegradability [1,7,12,13].

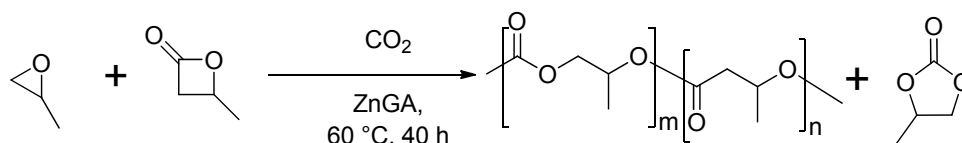
The copolymerization of epoxides and CO<sub>2</sub> was first reported by Tsuruta and Inoue [2,3] in 1969, since when a variety of homogeneous and heterogeneous catalysts have been developed for the copolymerization of CO<sub>2</sub> and epoxides [7,14–25]. Among these catalysts, zinc glutarate (ZnGA) has been widely employed as a heterogeneous catalyst in industry because it is economical and nontoxic, can be easily synthesized and dealt with, and affords high-molecular-weight copolymers [7,11,21,24,25].

In particular, ZnGA catalyzes the copolymerization of propylene oxide (PO) and CO<sub>2</sub> to afford poly(propylene carbonate) (PPC) with high molecular weight and a glass transition temperature ( $T_g$ ) of ~40 °C [7]. However, the thermal stability and biodegradability of PPC still remain to be enhanced for a wide range of industrial applications [7,13]. In this context, to modify the thermal and mechanical properties of the PPCs, the terpolymerization of PO and CO<sub>2</sub> with a third monomer has been presented as an economic and environmentally benign method [26–28]. To this end, ZnGA has been used as a catalyst in the terpolymerization of PO and CO<sub>2</sub> with several monomers, including lactones, cyclic anhydrides, and other epoxides [29–40].

Among them, lactones are interesting candidates because their ring opening polymerization affords the poly(hydroxyalkanoates) (PHA), a burgeoning class of thermoplastic polymers with enhanced biodegradability and thermal properties [41]. These PHA are useful in packaging films, drug release and biomedical implants [41–44]. Among these, the most common polyesters are the poly(3-hydroxy butyrates) (PHB), which are well known for their biocompatibility and biodegradability [45–48]. PHB can be inexpensively prepared by the ring opening polymerization of  $\beta$ -butyrolactone (BBL) [49–55].

Therefore, from an industrial point of view, including PHB segments in PPC would provide an opportunity to positively tune the mechanical and thermal properties and to enhance their biodegradability, thereby widening the applicability range of the both PHB and PPC. Here, using BBL as the third monomer in the ZnGA catalyzed copolymerization of PO and CO<sub>2</sub> could be envisaged as being a prolific method that would allow to insert PHB segments randomly in PPC. However, it was not until 2017 that the terpolymerization of an epoxide, CO<sub>2</sub>, and BBL was realized; indeed, BBL, despite its high ring strain, appears to be a less reactive monomer than higher lactones [45]. More recently, Rieger et al. [56] reported the homogeneous zinc-catalyzed one-pot synthesis of AB, ABA block terpolymers from BBL, cyclohexene oxide (CHO), and CO<sub>2</sub>, where the selectivity could be tuned by CO<sub>2</sub>.

From this background, the terpolymerization of PO, BBL, and CO<sub>2</sub> still remains to be achieved. Herein, as part of our continued research efforts to improve the catalytic activity of ZnGA and explore additional applications for ZnGA [11], we report the ZnGA-catalyzed terpolymerization of PO, BBL, and CO<sub>2</sub> (Scheme 1), which affords poly(ester-co-carbonates) with thermal and mechanical properties that can be tuned by adjusting the ratio of PO to BBL in the feedstock.



**Scheme 1.** Terpolymerization of PO, BBL, and CO<sub>2</sub> using ZnGA-20.

## 2. Results and Discussion

### 2.1. Synthesis and Characterization of Nano-Sized ZnGA

Nano-sized ZnGA (ZnGA-20) was prepared according to previous reports with slight modifications [6]. Briefly, glutaric acid (1.321 g, 10.0 mmol) was stirred in anhydrous toluene (20.0 mL) under a nitrogen atmosphere. Then, ZnO (0.814 g, 10.0 mmol) was introduced and the suspension was stirred at 20 °C for 24 h. The resulting white precipitates were then filtered and thoroughly washed with an excess of acetone before drying at 130 °C under vacuum for 12 h. The particles were then analyzed using powder X-ray diffraction (PXRD) and Fourier transform infrared (FT-IR) spectroscopy, scanning electron microscopy (SEM), and Brunauer–Emmett–Teller (BET) isotherm analysis. The PXRD pattern of the as-prepared ZnGA-20 and the pattern calculated from the crystal structure are compared in Figure 1a, which clearly shows all the typical reflexes for ZnGA, implying that ZnGA-20 and standard ZnGA share the same crystal lattice. Among all the reflexes, three strong reflexes at  $2\theta$  values of  $\sim 12.5^\circ$ ,  $\sim 22.5^\circ$ , and  $\sim 23.0^\circ$  were selected, and their Miller indices were found to be (200), (210), and (20–2), respectively. The coherence length ( $L_{c(hkl)}$ ), which is a measure of crystal quality, was calculated from the full width at half maximum (FWHM) values of the corresponding reflexes using Scherrer's equation, and the results are summarized in Table S1. The overall crystallinity ( $X_c$ ) of the catalyst was calculated to be 69.1% from the deconvoluted crystalline and amorphous regions of the PXRD pattern (Table S1).

The corresponding FT-IR spectroscopic analysis shows the typical bands for ZnGA (Figure 1b) [6]. Thus, the COO<sup>−</sup> antisymmetric stretching bands were observed at  $\sim 1584\text{ cm}^{-1}$  and  $\sim 1405\text{ cm}^{-1}$ ,

a  $\text{COO}^-$  symmetric stretching band was observed at  $1538\text{ cm}^{-1}$ , and the CH stretching and  $\text{CH}_2$  scissoring bands appeared at  $2955\text{ cm}^{-1}$  and  $1445\text{ cm}^{-1}$ , respectively. Figure 1c displays a SEM image of ZnGA-20, which exhibits nano-sized rectangular platelets with approximately  $80\text{ nm} \times 70\text{ nm}$  of length and width, respectively, and an average thickness lower than  $20\text{ nm}$ . Moreover, the BET isotherm analysis of ZnGA-20 shows that the catalyst is a mesoporous material with a mean pore size of  $32.4\text{ nm}$  and a surface area of  $22.7\text{ m}^2/\text{g}$ , being these values typical of ZnGA frameworks (Table S1).

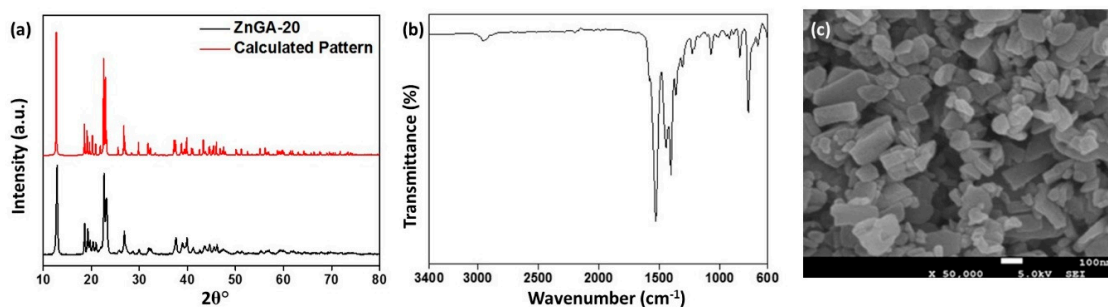


**Figure 1.** (a) PXRD pattern of ZnGA-20 and PXRD pattern calculated from the crystal structure of ZnGA via Mercury 3.7 [57], (b) FT-IR spectrum, and (c) SEM image of ZnGA-20.

## 2.2. Terpolymerization of PO, BBL, and $\text{CO}_2$ using ZnGA-20 as the Catalyst

With catalyst ZnGA-20 in hand, we set out to investigate its catalytic activity in the terpolymerization of PO,  $\text{CO}_2$ , and BBL under different reaction conditions. Initially, the terpolymerization was attempted with 30 equivalents of a 1:1 mixture of PO and BBL and 1 equivalent of ZnGA-20 at  $60^\circ\text{C}$  in the presence of  $1.5\text{ MPa}$  of  $\text{CO}_2$  for 40 h. The resulting reaction mixture was analyzed using  $^1\text{H-NMR}$  spectroscopy (Figure 2) to find that the formation of the expected terpolymer had occurred and was accompanied by a small amount of cyclic propylene carbonate (PC). It should be noted, here, that although some other metal organic framework (MOF) systems were reported to produce cyclic carbonates as a product in the reaction of  $\text{CO}_2$  with an epoxide, the ZnGA is the only MOF to produce poly(alkylene carbonate) as a major product [58–61].

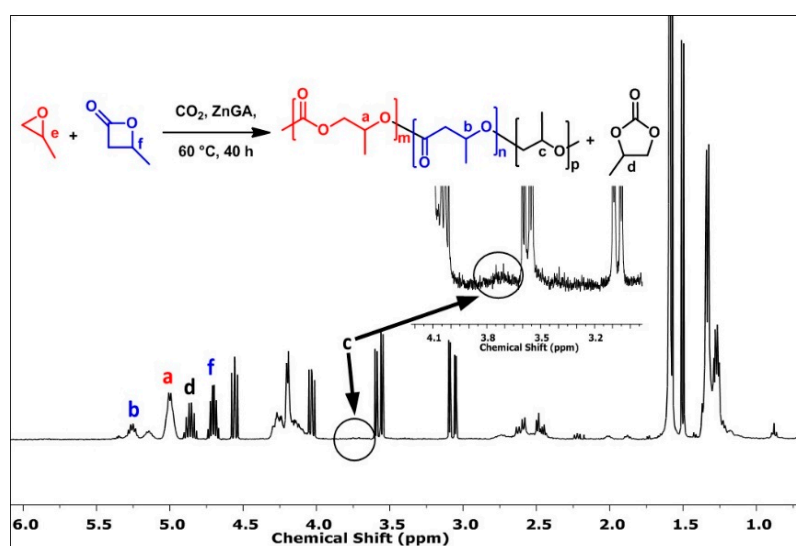


**Figure 2.**  $^1\text{H-NMR}$  spectrum of the mixture of poly(ester-co-carbonate) and cyclic carbonate obtained using the conditions of Entry 1, Table 1.

Thus, the methine protons of PHB, PPC, and PC gave rise to resonances located at  $5.4\text{--}5.1$ ,  $4.8\text{--}5.0$ , and  $4.8\text{ ppm}$ , respectively. Moreover, the small hump that can be observed at  $5.1\text{ ppm}$  is attributable to random PHB and PPC linkages.

From this spectrum, it can be concluded that a terpolymer of PO, BBL, and CO<sub>2</sub> was obtained with a very low turnover number (TON) of 7.3 g polymer/g catalyst (Entry 1, Table 1). Interestingly, this heterogeneous, one-pot system affords methanol-insoluble poly(ester-co-carbonates) with random linkages between PPC and PHB polymers. Following this initial success, the terpolymerization was systematically studied at a substrate to catalyst ratio (S/C) of 100 using different PO:BBL ratios (9:1, 3:1, 1:1, and 1:3). The results obtained are summarized in Table 1, and the <sup>1</sup>H-NMR spectra of the resulting polymers are shown in Figure S1.

As summarized in Table 1, the TON was found to decrease gradually with an increase the amount of BBL. The highest TON was observed for the infeed PO to BBL ratio of 3:1. Interestingly, the PHB content in the terpolymer increased with the amount of BBL in the feed, reaching a maximum of 29.0% when the feed ratio of PO to BBL was maintained as 1:3 (Entry 5, Table 1). These results suggested that by controlling the PPC/PHB ratio in the resulting polymers, their thermal and mechanical properties might be tuned.

Among the screened reactions, the highest TON of 24.6 g polymer/g catalyst was obtained when the infeed ratio of PO to BBL was 3:1, which afforded lactone and PO conversions of 22.4% and 54.6%, respectively (Entry 3, Table 1). Next, the S/C ratio was increased to 270, a ratio that was used in the regular copolymerization of PO and CO<sub>2</sub>, and the feed ratio of PO to BBL was set to 0.75:0.25 with 1.5 MPa of CO<sub>2</sub>.

**Table 1.** Terpolymerization of PO, CO<sub>2</sub>, and BBL using ZnGA-20 <sup>a</sup>.

Entry	Zn:PO:BBL	CO <sub>2</sub> (MPa)	TON <sup>b</sup>	Conversion (%) <sup>c</sup>		PPC (%)	PHB (%)	PE (%) <sup>d</sup>	M <sub>n</sub> (kg/mol) <sup>e</sup>	PDI <sup>e</sup>	T <sub>g</sub> (°C) <sup>f</sup>	T <sub>5%</sub> (°C) <sup>g</sup>
				PO	BBL							
1 <sup>h</sup>	1:15:13	1.5	7.3	58.0	46.5	62.0	36.0	2.5	–	–	–	–
2	1:90:10	1.5	24.0	47.4	21.6	93.0	4.0	3.0	69.8	3.7	37	183.4
3	1:75:25	1.5	24.6	54.6	22.4	87.0	10.0	3.0	45.1	3.5	34	209.9
4	1:50:50	1.5	18.5	58.1	12.6	82.0	15.0	2.0	41.4	4.9	30	206.1
5	1:25:75	1.5	9.5	48.6	8.3	67.0	29.0	3.0	25.9	5.6	20	231.9
6	1:202.5:67.5	1.5	60.8	49.4	22.4	86.0	11.0	4.0	127.5	2.5	34	224.2
7	1:135:135	1.5	67.5	78.5	19.3	82.0	17.0	2.0	83.5	2.6	35	242.2
8	1:202.5:67.5	3.0	74.4	62.5	25.0	88.0	10.0	2.0	123.0	2.6	41	212.8
9 <sup>i</sup>	1:202.5:67.5	15	na	0.0	0.0	nd	nd	nd	na	na	na	na

<sup>a</sup> Reaction condition: 0.05 g of catalyst, 60 °C, and 40 h. <sup>b</sup> TON: g of polymer/g of catalyst, calculated from the resulting polymer. <sup>c</sup> Conversion into the polymeric product. <sup>d</sup> PE = polyether; <sup>e</sup> M<sub>n</sub>, M<sub>w</sub>, and polydispersity index (PDI) values of the polymers were determined using gel permeation chromatography (GPC) with polystyrene standards in tetrahydrofuran (THF); PDI = M<sub>w</sub>/M<sub>n</sub>. <sup>f</sup> Obtained via differential scanning calorimetric (DSC) analysis. <sup>g</sup> Obtained via thermogravimetric analysis (TGA) analysis. <sup>h</sup> 0.2 g of ZnGA is used. <sup>i</sup> Reaction was performed in the absence of catalyst; nd = not detected; na = not applicable.

As expected, the TON was found to increase remarkably to 60.8 g polymer/g catalyst, and the corresponding polymer contained PPC and PHB units in an 8:1 ratio (Entry 6, Table 1). The conversions of the monomers PO and BBL reached values similar to those obtained using an S/C ratio of 100, i.e., 49.4% and 22.4%, respectively, thereby demonstrating the catalytic nature of the process. Surprisingly, increasing the BBL content to 50% in feed under similar conditions led to a significant increment in the TON, along with an improvement of the PO conversion to 78.5% (Entry 7, Table 1). Finally, the CO<sub>2</sub> pressure also had an influence on the reaction, as can be seen in Entry 8, Table 1. Thus, when the PO to BBL ratio was maintained at 0.75:0.25 with an S/C ratio of 270, increasing the CO<sub>2</sub> pressure to 3.0 MPa afforded the highest TON of 74.4, and the PPC to PHB ratio in the resultant polymer was found to be 9:1. Furthermore, the conversion rates of PO and BBL were found to increase to 62.5% and 25%, respectively. Finally, a blank experiment in the absence of catalyst was performed in which no product formation was observed and both PO and BBL were found to remain unchanged after the reaction indicating the true catalytic nature of the reaction (Entry 9, Table 1).

### 2.3. Properties of the Terpolymers

The terpolymers obtained were subjected to GPC analysis, and the representative GPC elugrams of the terpolymers from Entry 7 and Entry 8 are shown in Figure 3a. Interestingly, broad curves with large PDI values were observed in the elugrams. The unimodal distribution curves show that the polymers were formed as random copolymers of the PPC and PHB units. The small hump at 5.1 ppm in the  $^1\text{H-NMR}$  spectra of the polymers also suggests that the polymers had random PPC and PHB linkages. (Figure 3a and Figure S1). The  $M_n$  values of the terpolymers were low when the S/C ratio was maintained at 100, whereas high-molecular-weight polymers were formed in the case of S/C = 270. Moreover, the  $M_n$  value was found to increase with the PPC content in the polymers.

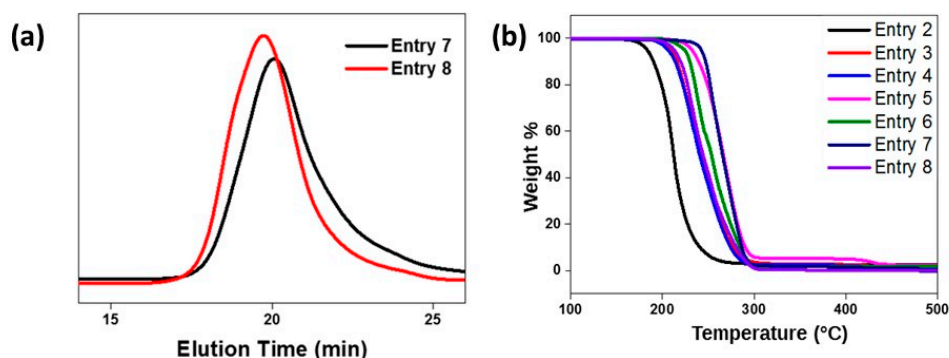


**Figure 3.** (a) GPC elugrams of the terpolymers corresponding to Entries 2–8 in Table 1; (b) TGA curves of the poly(ester-co-carbonates) obtained from Entries 2–8 in Table 1.

The thermal stability and  $T_g$  of the terpolymers were then determined using TGA and DSC analyses. The 5% decomposition temperature values ( $T_{5\%}$ ) for the polymers were obtained from the TGA curves and are listed in Table 1. Figure 3b shows the TGA curves of the obtained polymers corresponding to Entries 2–8 in Table 1. As expected, the thermal stability of the polymers increased with the PHB content. From Entries 6–8, it is evident that the polymer from Entry 7 with higher PHB content shows the highest  $T_{5\%}$  value. The  $T_g$  value of the terpolymers decreased when the PHB content increased, and the lowest  $T_g$  value of 20 °C was obtained for the polymer with the maximum PHB content of 29% (Table 1).

### 3. Materials and Methods

ZnO (99.99%) and BBL (1.25 M) were purchased from Sigma–Aldrich (Seoul, Korea) and were used as received. Glutaric acid ( $\geq 99.0\%$ ) was obtained from Tokyo Chemical Industry Co., Ltd. (Tokyo, Japan) and was used without further purification. Propylene oxide ( $\geq 99.9\%$ ) was received from Sigma–Aldrich (Seoul, Korea) and was distilled over  $\text{CaH}_2$  before use. High-purity  $\text{CO}_2$  gas was obtained from Shinyang Gas Industries (Paju-si, Korea) and was used as received.

The morphologies of the as-prepared catalysts were characterized by field emission scanning electron microscopy (a Hitachi FE-SEM S-4800, Tokyo, Japan). Powder X-ray diffraction (PXRD) measurements were performed at room temperature using a X-Ray Diffractometer system (D/MAX-2500V) Rigaku, (Tokyo, Japan) using  $\text{CuK}\alpha$  radiation. Fourier-transform infrared (FT-IR) spectra were obtained on a Nicolet iS 50 (Thermo Fisher Scientific, Waltham, MA, USA) spectrometer that was equipped with an attenuated total reflectance (ATR) accessory at room temperature. Metal content in ZnGA-20 was determined by inductively coupled plasma atomic emission spectroscopy (ICP-OES) (iCAP-Q, Thermo Fisher Scientific, Waltham, MA, USA) using microwave assisted acid digestion system (MARS6, CEM/USA, (Waltham, MA, USA)). The  $\text{N}_2$  adsorption–desorption measurements were conducted using an automated gas sorption system (Belsorp II mini, BEL Japan, Inc., Tokyo, Japan) at 77 K. The samples were degassed for 12 h at 130 °C before performing the measurement. The Barrett–Joyner–Halenda (BJH) method was used to

assess the pore size distribution. The  $^1\text{H-NMR}$  spectra of the products were obtained using a Bruker Ascend 400 MHz spectrometer (Rheinstetten, Germany). Thermogravimetric analysis (TGA) was performed using a 2960 Simultaneous DSC-TGA instrument (TA instruments, New Castle, DE, USA) at a heating rate of  $10\text{ }^\circ\text{C}/\text{min}$  from  $25\text{ }^\circ\text{C}$  to  $500\text{ }^\circ\text{C}$  under a nitrogen atmosphere. Differential scanning calorimetric (DSC) tests were performed on a PerkinElmer DSC 4000 instrument (Waltham, MA, USA) at a heating rate of  $10\text{ }^\circ\text{C}/\text{min}$  from  $-40\text{ }^\circ\text{C}$  to  $120\text{ }^\circ\text{C}$  under a nitrogen atmosphere. The molecular weights and polydispersity index of the polymers were determined by gel permeation chromatography (GPC) using a Waters 717plus instrument (Milford, MA, USA) that was equipped with a Waters 515 HPLC pump (Massachusetts, United States). The columns were eluted with THF at a flow rate of  $1.00\text{ mL}/\text{min}$  at  $35\text{ }^\circ\text{C}$ . The GPC curves were calibrated using polystyrene standards with molecular weight ranging from 580 to 660,500.

### 3.1. Synthesis of ZnGA-20

Glutaric acid (1.321 g, 10.0 mmol) and ZnO (0.814 g, 10.0 mmol) were charged into a glass-autoclave reactor followed by 20.0 mL anhydrous toluene under Ar atmosphere. The resulting white suspension was stirred at  $20\text{ }^\circ\text{C}$  for 24 h. After 24 h, the reaction mixture was filtered off, washed with excess of acetone ( $50.0\text{ mL} \times 5$ ), and dried under vacuum at  $130\text{ }^\circ\text{C}$  to yield 1.910 g of ZnGA-20 (Yield = 97.6%). The content of Zn in the catalyst was estimated to be approximately 33.4 wt.% by ICP-OES.

### 3.2. General Procedure for the Copolymerization of $\text{CO}_2$ and PO

All terpolymerization reactions were carried out in a pre-dried 100 mL stainless steel autoclave reactor equipped with a magnetic stirrer and a programmable temperature controller. In a typical reaction, the desired amounts of catalyst, PO, and BBL were added under Ar atmosphere and then pressurized with  $\text{CO}_2$  to 1.5 MPa at room temperature. The mixture was stirred at  $60\text{ }^\circ\text{C}$  for 40 h. After cooling the reactor to room temperature,  $\text{CO}_2$  was slowly released. A small fraction was taken for  $^1\text{H NMR}$  analysis and the remaining mass was dissolved in dichloromethane (5.0 mL) and was treated with 1.25 M methanolic HCl solution ( $20.0\text{ mL} \times 3$ ). Addition of excess methanol ( $\sim 50.0\text{ mL}$ ) to the solution afforded the polymer as a white precipitate and was dried under vacuum at  $60\text{ }^\circ\text{C}$  for 12 h.

## 4. Conclusions

The terpolymerization of PO, BBL, and  $\text{CO}_2$  was achieved for the first time using the heterogeneous nano-sized catalyst ZnGA-20. The reactivity of both PO and BBL was found to increase when increasing the  $\text{CO}_2$  pressure. Furthermore, the polyester incorporation into the poly(carbonate-co-ester), which reached a maximum of 29%, could be tuned by adjusting the feed ratio of PO to BBL. The thermal stability of the terpolymers increased, whereas  $T_g$  decreased, when the PHB content increased.

**Supplementary Materials:** The following are available online at <http://www.mdpi.com/2073-4344/8/9/393/s1>, Figure S1:  $^1\text{H-NMR}$  spectra of the polymers produced using the conditions described in Entries 2–8, Table 1 of the main text. Table S1: PXRD and BET data of ZnGA-20.

**Author Contributions:** Conceptualization, S.P. and S.Y.; Formal Analysis, S.P. and S.D.; Investigation, S.P.; Writing–Original Draft Preparation, S.P.; Supervision, S.Y.

**Acknowledgments:** We acknowledge the financial support through grants from the Korea CCS R&D Center, funded by the Ministry of Education, Science and Technology of the Korean Government (No. 2014M1A8A1049300).

**Conflicts of Interest:** The authors declare no conflict of interest.

## References

1. Scharfenberg, M.; Hilf, J.; Frey, H. Functional polycarbonates from carbon dioxide and tailored epoxide monomers: Degradable materials and their application potential. *Adv. Funct. Mater.* **2018**. [CrossRef]

2. Inoue, S.; Koinuma, H.; Tsuruta, T. Copolymerization of carbon dioxide and epoxide. *J. Polym. Sci. B Polym. Lett.* **1969**, *7*, 287–292. [[CrossRef](#)]
3. Inoue, S.; Koinuma, H.; Tsuruta, T. Copolymerization of carbon dioxide and epoxide with organometallic compounds. *Makromolekul. Chem.* **1969**, *130*, 210–220. [[CrossRef](#)]
4. Soga, K.; Imai, E.; Hattori, I. Alternating copolymerization of CO<sub>2</sub> and propylene-oxide with the catalysts prepared from Zn(OH)<sub>2</sub> and various dicarboxylic-acids. *Polym. J.* **1981**, *13*, 407–410. [[CrossRef](#)]
5. Darensbourg, D.J.; Stafford, N.W.; Katsurao, T. Supercritical carbon-dioxide as solvent for the copolymerization of carbon-dioxide and propylene-oxide using a heterogeneous zinc carboxylate catalyst. *J. Mol. Catal. A Chem.* **1995**, *104*, L1–L4. [[CrossRef](#)]
6. Ree, M.; Bae, J.Y.; Jung, J.H.; Shin, T.J. A new copolymerization process leading to poly(propylene carbonate) with a highly enhanced yield from carbon dioxide and propylene oxide. *J. Polym. Sci. A Polym. Chem.* **1999**, *37*, 1863–1876. [[CrossRef](#)]
7. Luinstra, G.A. Poly(propylene carbonate), old copolymers of propylene oxide and carbon dioxide with new interests: Catalysis and material properties. *Polym. Rev.* **2008**, *48*, 192–219. [[CrossRef](#)]
8. Ang, R.R.; Sin, L.T.; Bee, S.T.; Tee, T.T.; Kadhum, A.A.H.; Rahmat, A.R.; Wasmi, B.A. Determination of zinc glutarate complexes synthesis factors affecting production of propylene carbonate from carbon dioxide and propylene oxide. *Chem. Eng. J.* **2017**, *327*, 120–127. [[CrossRef](#)]
9. Scott, D.A.; Christopher, M.B.; Geoffrey, W.C. Carbon dioxide as a renewable C1 feedstock: Synthesis and characterization of polycarbonates from the alternating copolymerization of epoxides and CO<sub>2</sub>. In *Feedstocks for the Future*; Joseph, J.B., Martin, K.P., Eds.; American Chemical Society: Washington, DC, USA, 2006; Chapter 9; Volume 921, pp. 116–129.
10. Van der Assen, N.; Bardow, A. Life cycle assessment of polyols for polyurethane production using CO<sub>2</sub> as feedstock: Insights from an industrial case study. *Green Chem.* **2014**, *16*, 3272–3280. [[CrossRef](#)]
11. Sudakar, P.; Sivanesan, D.; Yoon, S. Copolymerization of epichlorohydrin and CO<sub>2</sub> using zinc glutarate: An additional application of ZnGA in polycarbonate synthesis. *Macromol. Rapid Commun.* **2016**, *37*, 788–793. [[CrossRef](#)] [[PubMed](#)]
12. Luinstra, G.A.; Haas, G.R.; Molnar, F.; Bernhart, V.; Eberhardt, R.; Rieger, B. On the formation of aliphatic polycarbonates from epoxides with chromium (iii) and aluminum (iii) metal-salen complexes. *Chem.-Eur. J.* **2005**, *11*, 6298–6314. [[CrossRef](#)] [[PubMed](#)]
13. Luinstra, G.A.; Borchardt, E. Material properties of poly(propylene carbonates). *Adv. Polym. Sci.* **2012**, *245*, 29–48.
14. Kobayashi, M.; Inoue, S.; Tsuruta, T. Diethylzinc-dihydric phenol system as catalyst for copolymerization of carbon dioxide with propylene oxide. *Macromolecules* **1971**, *4*, 658–659. [[CrossRef](#)]
15. Inoue, S.; Tsuruta, T.; Kobayashi, M.; Koinuma, H. Reactivities of some organozinc initiators for copolymerization of carbon-dioxide and propylene oxide. *Makromolekul. Chem.* **1972**, *155*. [[CrossRef](#)]
16. Kobayashi, M.; Inoue, S.; Tsuruta, T. Copolymerization of carbon-dioxide and epoxide by dialkylzinc-carboxylic acid system. *J. Polym. Sci. A Polym. Chem.* **1973**, *11*, 2383–2385. [[CrossRef](#)]
17. Kobayashi, M.; Tang, Y.L.; Tsuruta, T.; Inoue, S. Copolymerization of carbon-dioxide and epoxide using dialkylzinc-dihydric phenol system as catalyst. *Makromol. Chem.* **1973**, *169*, 69–81. [[CrossRef](#)]
18. Kuran, W.; Pasynkiewicz, S.; Skupinska, J. Investigations on catalytic systems diethylzinc-dihydroxybenzenes and trihydroxybenzenes in copolymerization of carbon-dioxide with propylene-oxide. *Makromol. Chem.* **1976**, *177*, 1283–1292. [[CrossRef](#)]
19. Kuran, W.; Pasynkiewicz, S.; Skupinska, J.; Rokicki, A. Alternating copolymerization of carbon-dioxide and propylene-oxide in presence of organometallic catalysts. *Makromol. Chem.* **1976**, *177*, 11–20. [[CrossRef](#)]
20. Soga, K.; Uenishi, K.; Hosoda, S.; Ikeda, S. Copolymerization of carbon-dioxide and propylene-oxide with new catalysts. *Makromol. Chem.* **1977**, *178*, 893–897. [[CrossRef](#)]
21. Darensbourg, D.J. Making plastics from carbon dioxide: Salen metal complexes as catalysts for the production of polycarbonates from epoxides and CO<sub>2</sub>. *Chem. Rev.* **2007**, *107*, 2388–2410. [[CrossRef](#)] [[PubMed](#)]
22. Darensbourg, D.J.; Fitch, S.B. (tetramethyltetraazaannulene) chromium chloride: A highly active catalyst for the alternating copolymerization of epoxides and carbon dioxide. *Inorg. Chem.* **2007**, *46*, 5474–5476. [[CrossRef](#)] [[PubMed](#)]
23. Darensbourg, D.J.; Frantz, E.B. Manganese(III) schiff base complexes: Chemistry relevant to the copolymerization of epoxides and carbon dioxide. *Inorg. Chem.* **2007**, *46*, 5967–5978. [[CrossRef](#)] [[PubMed](#)]

24. Ang, R.R.; Sin, L.T.; Bee, S.T.; Tee, T.T.; Kadhum, A.A.H.; Rahmat, A.R.; Wasmi, B.A. A review of copolymerization of green house gas carbon dioxide and oxiranes to produce polycarbonate. *J. Clean. Prod.* **2015**, *102*, 1–17. [[CrossRef](#)]
25. Trott, G.; Saini, P.K.; Williams, C.K. Catalysts for CO<sub>2</sub>/epoxide ring-opening copolymerization. *Philos. Trans. R. Soc. A* **2016**. [[CrossRef](#)] [[PubMed](#)]
26. Paul, S.; Romain, C.; Shaw, J.; Williams, C.K. Sequence selective polymerization catalysis: A new route to abablock copoly(ester-b-carbonate-b-ester). *Macromolecules* **2015**, *48*, 6047–6056. [[CrossRef](#)]
27. Romain, C.; Zhu, Y.; Dingwall, P.; Paul, S.; Rzepa, H.S.; Buchard, A.; Williams, C.K. Chemoselective polymerizations from mixtures of epoxide, lactone, anhydride, and carbon dioxide. *J. Am. Chem. Soc.* **2016**, *138*, 4120–4131. [[CrossRef](#)] [[PubMed](#)]
28. Romain, C.; Williams, C.K. Chemoselective polymerization control: From mixed-monomer feedstock to copolymers. *Angew. Chem. Int. Ed.* **2014**, *53*, 1607–1610. [[CrossRef](#)] [[PubMed](#)]
29. Hwang, Y.T.; Jung, J.W.; Ree, M.; Kim, H. Terpolymerization of CO<sub>2</sub> with propylene oxide and epsilon-caprolactone using zinc glutarate catalyst. *Macromolecules* **2003**, *36*, 8210–8212. [[CrossRef](#)]
30. Ree, M.; Hwang, Y.; Kim, J.S.; Kim, H.; Kim, G.; Kim, H. New findings in the catalytic activity of zinc glutarate and its application in the chemical fixation of CO<sub>2</sub> into polycarbonates and their derivatives. *Catal. Today* **2006**, *115*, 134–145. [[CrossRef](#)]
31. Zou, Y.N.; Xiao, M.; Li, X.H.; Wang, S.J.; Meng, Y.Z. Biodegradability enhanced terpolymer of propylene oxide and ethylene oxide with carbon dioxide using zinc glutarate as catalyst. *Polym. Polym. Compos.* **2007**, *15*, 53–58. [[CrossRef](#)]
32. Song, P.F.; Xiao, M.; Du, F.G.; Wang, S.J.; Gan, L.Q.; Liu, G.Q.; Meng, Y.Z. Synthesis and properties of aliphatic polycarbonates derived from carbon dioxide, propylene oxide and maleic anhydride. *J. Appl. Polym. Sci.* **2008**, *109*, 4121–4129. [[CrossRef](#)]
33. Song, P.F.; Wang, S.J.; Xiao, M.; Du, F.G.; Gan, L.Q.; Liu, G.Q.; Meng, Y.Z. Cross-linkable and thermally stable aliphatic polycarbonates derived from CO<sub>2</sub>, propylene oxide and maleic anhydride. *J. Polym. Res.* **2009**, *16*, 91–97. [[CrossRef](#)]
34. Wu, J.S.; Xiao, M.; He, H.; Wang, S.J.; Han, D.M.; Meng, Y.Z. Copolymerization of propylene oxide and carbon dioxide in the presence of diphenylmethane diisocyanate. *J. Polym. Res.* **2011**, *18*, 1479–1486. [[CrossRef](#)]
35. Liu, Y.L.; Xiao, M.; Wang, S.J.; Xia, L.; Hang, D.M.; Cui, G.F.; Meng, Y.Z. Mechanism studies of terpolymerization of phthalic anhydride, propylene epoxide, and carbon dioxide catalyzed by ZnGa. *RSC Adv.* **2014**, *4*, 9503–9508. [[CrossRef](#)]
36. Nornberg, B.; Luinstra, G.A. Influence of norbornene dicarboxylic anhydride on the copolymerization of carbon dioxide and propylene oxide. *Eur. Polym. J.* **2015**, *73*, 297–307. [[CrossRef](#)]
37. Tang, L.; Luo, W.H.; Xiao, M.; Wang, S.J.; Meng, Y.Z. One-pot synthesis of terpolymers with long l-lactide rich sequence derived from propylene oxide, CO<sub>2</sub>, and l-lactide catalyzed by zinc adipate. *J. Polym. Sci. Pol. A Chem.* **2015**, *53*, 1734–1741. [[CrossRef](#)]
38. Luo, W.H.; Xiao, M.; Wang, S.J.; Han, D.M.; Meng, Y.Z. Gradient terpolymers with long epsilon-caprolactone rich sequence derived from propylene oxide, CO<sub>2</sub>, and epsilon-caprolactone catalyzed by zinc glutarate. *Eur. Polym. J.* **2016**, *84*, 245–255. [[CrossRef](#)]
39. Song, P.F.; Xu, H.D.; Mao, X.D.; Liu, X.J.; Wang, L. A one-step strategy for aliphatic poly(carbonate-ester)s with high performance derived from CO<sub>2</sub>, propylene oxide and l-lactide. *Polym. Adv. Technol.* **2017**, *28*, 736–741. [[CrossRef](#)]
40. Hwang, Y.; Kim, H.; Ree, M. Zinc glutarate catalyzed synthesis and biodegradability of poly(carbonate-co-ester)s from CO<sub>2</sub>, propylene oxide, and epsilon-caprolactone. *Macromol. Symp.* **2005**, *224*, 227–237. [[CrossRef](#)]
41. Uhrich, K.E.; Cannizzaro, S.M.; Langer, R.S.; Shakesheff, K.M. Polymeric systems for controlled drug release. *Chem. Rev.* **1999**, *99*, 3181–3198. [[CrossRef](#)] [[PubMed](#)]
42. Sudesh, K.; Abe, H.; Doi, Y. Synthesis, structure and properties of polyhydroxyalkanoates: Biological polyesters. *Prog. Polym. Sci.* **2000**, *25*, 1503–1555. [[CrossRef](#)]
43. Mecking, S. Nature or petrochemistry? Biologically degradable materials. *Angew. Chem. Int. Ed.* **2004**, *43*, 1078–1085. [[CrossRef](#)] [[PubMed](#)]
44. Li, Z.B.; Yang, J.; Loh, X.J. Polyhydroxyalkanoates: Opening doors for a sustainable future. *NPG Asia Mater.* **2016**, *8*, e265. [[CrossRef](#)]



45. Carpentier, J.-F. Discrete metal catalysts for stereoselective ring-opening polymerization of chiral racemic  $\beta$ -lactones. *Macromol. Rapid Commun.* **2010**, *31*, 1696–1705. [[CrossRef](#)] [[PubMed](#)]
46. Thomas, C.M. Stereocontrolled ring-opening polymerization of cyclic esters: Synthesis of new polyester microstructures. *Chem. Soc. Rev.* **2010**, *39*, 165–173. [[CrossRef](#)] [[PubMed](#)]
47. Holmes, P.A. Applications of phb—A microbially produced biodegradable thermoplastic. *Phys. Technol.* **1985**, *16*, 32–36. [[CrossRef](#)]
48. Okada, M. Chemical syntheses of biodegradable polymers. *Prog. Polym. Sci.* **2002**, *27*, 87–133. [[CrossRef](#)]
49. Rieth, L.R.; Moore, D.R.; Lobkovsky, E.B.; Coates, G.W. Single-site beta-diiminate zinc catalysts for the ring-opening polymerization of beta-butyrolactone and beta-valerolactone to poly(3-hydroxyalkanoates). *J. Am. Chem. Soc.* **2002**, *124*, 15239–15248. [[CrossRef](#)] [[PubMed](#)]
50. Kramer, J.W.; Coates, G.W. Fluorinated beta-lactones and poly(beta-hydroxyalkanoate)s: Synthesis via epoxide carbonylation and ring-opening polymerization. *Tetrahedron* **2008**, *64*, 6973–6978. [[CrossRef](#)] [[PubMed](#)]
51. Kramer, J.W.; Treitler, D.S.; Dunn, E.W.; Castro, P.M.; Roisnel, T.; Thomas, C.M.; Coates, G.W. Polymerization of enantiopure monomers using syndiospecific catalysts: A new approach to sequence control in polymer synthesis. *J. Am. Chem. Soc.* **2009**, *131*, 16042–16044. [[CrossRef](#)] [[PubMed](#)]
52. Brule, E.; Gaillard, S.; Rager, M.N.; Roisnel, T.; Guerineau, V.; Nolan, S.P.; Thomas, C.M. Polymerization of racemic beta-butyrolactone using gold catalysts: A simple access to biodegradable polymers. *Organometallics* **2011**, *30*, 2650–2653. [[CrossRef](#)]
53. Ebrahimi, T.; Aluthge, D.C.; Hatzildriakos, S.G.; Mehrkhodavandi, P. Highly active chiral zinc catalysts for immortal polymerization of beta-butyrolactone from melt processable syndio-rich poly(hydroxybutyrate). *Macromolecules* **2016**, *49*, 8812–8824. [[CrossRef](#)]
54. Rajendiran, S.; Natarajan, P.; Yoon, S. A covalent triazine framework-based heterogenized al-co bimetallic catalyst for the ring-expansion carbonylation of epoxide to beta-lactone. *RSC Adv.* **2017**, *7*, 4635–4638. [[CrossRef](#)]
55. Rajendiran, S.; Park, G.; Yoon, S. Direct conversion of propylene oxide to 3-hydroxy butyric acid using a cobalt carbonyl ionic liquid catalyst. *Catalysts* **2017**, *7*, 228. [[CrossRef](#)]
56. Kernbichl, S.; Reiter, M.; Adams, F.; Vagin, S.; Rieger, B. CO<sub>2</sub>-controlled one-pot synthesis of AB, ABA block, and statistical terpolymers from  $\beta$ -butyrolactone, epoxides, and CO<sub>2</sub>. *J. Am. Chem. Soc.* **2017**, *139*, 6787–6790. [[CrossRef](#)] [[PubMed](#)]
57. Zheng, Y.Q.; Lin, J.L.; Zhang, H.L. Crystal structure of zinc glutarate, Zn(C<sub>5</sub>H<sub>6</sub>H<sub>4</sub>). *Z. Krist.-New Cryst. Struct.* **2000**, *215*, 535–536.
58. Jiang, Z.-R.; Wang, H.; Hu, Y.; Lu, J.; Jiang, H.-L. Polar group and defect engineering in a metal–organic framework: Synergistic promotion of carbon dioxide sorption and conversion. *ChemSusChem* **2015**, *8*, 878–885. [[CrossRef](#)] [[PubMed](#)]
59. Toyao, T.; Fujiwaki, M.; Miyahara, K.; Kim, T.-H.; Horiuchi, Y.; Matsuoka, M. Design of zeolitic imidazolate framework derived nitrogen-doped nanoporous carbons containing metal species for carbon dioxide fixation reactions. *ChemSusChem* **2015**, *8*, 3905–3912. [[CrossRef](#)] [[PubMed](#)]
60. Ding, M.; Chen, S.; Liu, X.-Q.; Sun, L.-B.; Lu, J.; Jiang, H.-L. Metal–organic framework-templated catalyst: Synergy in multiple sites for catalytic CO<sub>2</sub> fixation. *ChemSusChem* **2017**, *10*, 1898–1903. [[CrossRef](#)] [[PubMed](#)]
61. Cao, C.-S.; Shi, Y.; Xu, H.; Zhao, B. A multifunctional mof as a recyclable catalyst for the fixation of CO<sub>2</sub> with aziridines or epoxides and as a luminescent probe of cr(vi). *Dalton Trans.* **2018**, *47*, 4545–4553. [[CrossRef](#)] [[PubMed](#)]

